Breakdown of the Bloch-wave behavior for a single hole in a gapped antiferromagnet

Zheng Zhu,[1,2] D. N. Sheng,[3] and Zheng-Yu Weng[1,4]

[1]*Institute for Advanced Study, Tsinghua University, Beijing, 100084, China*
[2]*Department of Physics, Massachusetts Institute of Technology, Cambridge, MA, 02139, USA*
[3]*Department of Physics and Astronomy, California State University, Northridge, CA, 91330, USA*
[4]*Collaborative Innovation Center of Quantum Matter, Tsinghua University, Beijing, 100084, China*

(Dated: January 6, 2016)

Whether a doped hole propagates as a Bloch wave or not is an important issue of doped Mott physics. Here we examine this problem based on the quasiparticle spectral weight Z distribution, calculated by density matrix renormalization group (DMRG). By tuning the anisotropy of a two-leg t-J ladder without closing the background spin gap, the Z distribution unambiguously reveals a transition of the single hole state from a Bloch wave to a novel one with spontaneous translational symmetry breaking. We further establish a direct connection of such a transition with a nonlocal phase string entanglement between the hole and quantum spins, which explains numerical observations.

PACS numbers: 71.27.+a, 71.10.Fd

For a weakly interacting band insulator, a doped charge behaves like a Bloch wave in the presence of a periodic lattice obeying the Bloch theorem. One may also ask a meaningful question concerning the fate of a hole injected into a Mott insulator with correlated quantum spins[1,2]. For the special case that such a spin system is gapped and translationally invariant, based on the conventional wisdom, the doped hole would be expected to only disturb its surrounding spins to form some sort of spin polaron[2–6]. One might be tempted to generally conclude a Bloch-wave behavior for such a hole doping into a gapped spin system.

However, recent density matrix renormalization group (DMRG) studies[7–10] of hole-doped two-leg spin ladders have revealed an unexpected rich phenomenon even if the undoped system remains gapped. Although an injected hole does propagate like a simple Bloch wave in the strong anisotropic limit of the model, it undergoes a quantum transition to a novel state when the anisotropy is reduced. After the transition, the charge loses its phase coherence over a finite length scale[7,9], concomitant with an emergent interference pattern[10] (charge modulation) breaking the translational symmetry. Besides, a strong pairing of two holes also has been found[8] in this regime.

Nevertheless, in a recent new DMRG study of the same model, White, Scalapino, and Kivelson (WSK) claimed[11] that the critical point seen in the above studies[7–10] only signals a qualitative change of the quasiparticle energy spectrum without changing the Bloch wave nature on the both sides. The WSK's conclusion is largely based on the *total* quasiparticle spectral weight $Z_{\rm tot}$ (to be defined below), which remains finite and smooth across the transition point in their DMRG calculation[11].

To resolve the above controversy, in this paper, we directly compute the quasiparticle spectral weight distribution by DMRG. Although $Z_{\rm tot}$ previously calculated by WSK can be indeed reproduced, we point out that it is not sufficient to conclude the Bloch-wave behavior of the doped hole. Rather, one has to further examine Z_k and Z_j, denoting the probabilities of the ground state projecting onto a bare-hole Bloch state at momentum k and site j, respectively. We determine

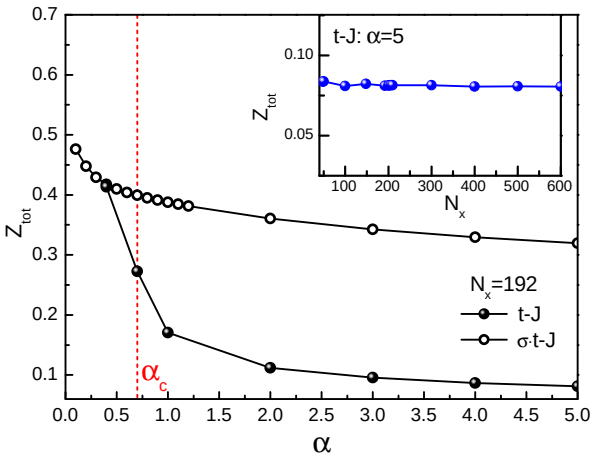

Fig. 1. (Color online). $Z_{\rm tot}$ measures the overlap of the true ground state of a single hole with a bare hole state [cf. Eq. (4)]. α denotes an anisotropic parameter for the two-leg t-J ladder. A critical point α_c is marked by the vertical dashed line, which is previously determined[9,10] by DMRG for the t-J case at $t/J = 3$ with $\alpha_c \approx 0.7$ (but there is no critical α_c for the so-called σ·t-J model, see text). Inset: the convergence of $Z_{\rm tot}$ with the sample size $N = N_x \times 2$ at $\alpha = 5$.

Z_k and Z_j, and show that the standard Bloch-wave behavior does break down on the one side of the aforementioned critical point, despite that $Z_{\rm tot}$ still remains finite and smooth. In particular, the length scale associated with the incoherence of the hole is identified from Z_j. We further derive an analytic formula serving as a direct probe of the underlying mechanism responsible for the charge incoherence and modulation, which is also verified by the DMRG calculation.

The model.— We study the one-hole ground state based on the standard two-leg t-J Hamiltonian composed of two one-dimensional chains (each with the hopping integral αt and the superexchange coupling αJ), which are coupled together by the hopping t and superexchange J at each rung to form a two-

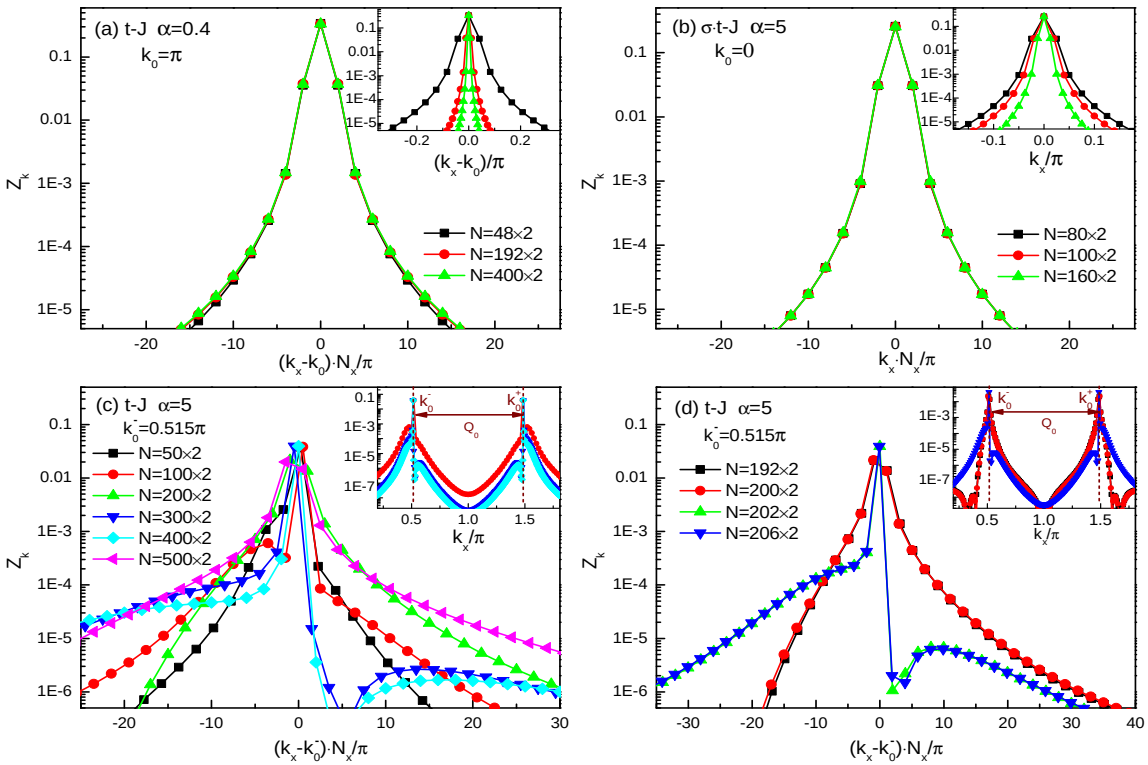

Fig. 2. (Color online). The quasiparticle spectral weight Z_k. Insets: the original Z_k's in different models with various sample lengths. Main panels: Bloch-wave quantization under the OBC as characterized by the scaling law with the k_x-axis replaced by $(k_x - k_0)N_x/\pi$. (a) The t-J case at $\alpha = 0.4 < \alpha_c$, a well-quantized Bloch wave with $k_0 = \pi$; (b) The σ·t-J ladder at $\alpha = 5$, a well-quantized Bloch wave with $k_0 = 0$; (c) and (d) The t-J case at $\alpha = 5 > \alpha_c$: although $Z_{\rm tot}$ as the total sum well converges (cf. the inset of Fig. 1), the quantization in a finite-size sample breaks down due to strong phase shifts occurring even at small variations of the sample length, for example, $N_x = 192$, 200, 202, and 206 [cf. (d)]. Here k_0 is split into two $k_0^{\pm}$ separated by an incommensurate Q_0 [cf. the insets of (c) and (d)].

leg ladder[7,9]. Here, the anisotropic parameter $\alpha \to 0$ in the strong rung limit, while two chains are decoupled at $\alpha \to \infty$. We focus on the model with $t/J = 3$, which is the same as studied in Refs. 7–10.

For the one-hole-doped t-J model, an exact expression of the partition function is given by[12]

$$\mathcal{Z}_{t\text{-}J} = \sum_c \tau_c \mathcal{W}[c] \,, \tag{1}$$

where the hole acquires a Berry-like phase[13] as

$$\tau_c = (-1)^{N_h^{\downarrow}[c]} = \pm 1 \tag{2}$$

along a closed path c (a brevity for multi-paths of the spins and the hole). Here $N_h^{\downarrow}[c]$ counts the total number of exchanges between the hole and down spins. The weight $\mathcal{W}[c] \geq 0$ is dependent on temperature $(1/\beta)$, t, J, and α[12]. The so-called σ·t-J model is introduced in Ref. 7 by inserting a spin-dependent sign in the hopping term of the t-J model, such that the one-hole partition function reduces to[7]

$$\mathcal{Z}_{\sigma\cdot t\text{-}J} = \sum_c \mathcal{W}[c] \,, \tag{3}$$

which is different from $\mathcal{Z}_{t\text{-}J}$ [Eq. (1)] only by the absence of the Berry-like phase τ_c, with the same $\mathcal{W}[c]$.

In the following, we shall study both models in a comparative way by using the DMRG algorithm[7–11]. For these calculations, we keep up to around 1800 states, which controls the truncation error to be in the order of 10^{-10} and 10^{-6} for open and periodic systems, respectively. For Z_j calculations, we do more than 200 sweeps to obtain well converged results.

The quasiparticle spectral weight.— The *total* quasiparticle spectral weight is defined by

$$Z_{\rm tot} \equiv \sum_k Z_k \equiv \sum_j Z_j \,, \tag{4}$$

where $Z_k \equiv |\langle \mathbf{k}|\Psi_G\rangle|^2$ or $Z_j \equiv |\langle j|\Psi_G\rangle|^2$ denotes the probability of the ground state $|\Psi_G\rangle$ in the bare hole Bloch state $|\mathbf{k}\rangle$ of momentum $\mathbf{k}$ or $|j\rangle$ at site j of coordinate $\mathbf{r}_j$. Here $|\mathbf{k}\rangle \equiv \frac{1}{\sqrt{2N_x}} \sum_j e^{i\mathbf{k}\cdot\mathbf{r}_j} |j\rangle$ and $|j\rangle \equiv \sqrt{2} c_j |\phi_0\rangle$ (with a proper normalization factor included), where $|\phi_0\rangle$ denotes the half-filling ground state. Note that $\mathbf{k} = (k_x, k_y)$ in general but we shall only focus on $k_y = 0$ case in the considered regime of the two-leg ladder where the $k_y = \pi$ component of the Z_k is exponentially small.

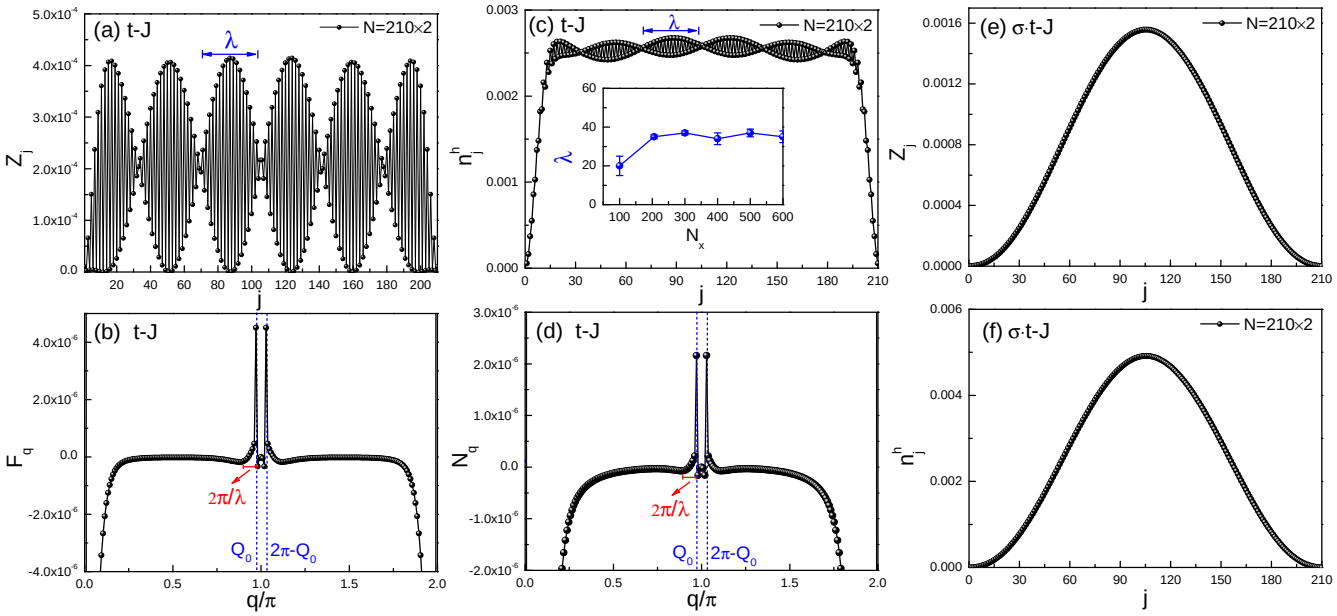

Fig. 3. (Color online). (a) Z_j measures the probability of a bare hole at site j, which shows a fast oscillation modulated by a slower variation at a length scale of λ ($\alpha = 5 > \alpha_c$); (b) The Fourier transformation of Z_j reveals the characteristic wave vector Q_0 with a continuous spread $\sim 2\pi/\lambda$; (c) and (d) The corresponding hole density distribution n_j^h and its Fourier transformation; Inset of (c): The length scale λ vs. N_x. Finally, smooth Z_j [(e)] and n_j^h [(f)] for the σ·t-J model at $\alpha = 5$.

$Z_{\rm tot}$ computed by DMRG is shown in Fig. 1, which is in good agreement with the WSK's result[11] for the t-J case. Note that $Z_{\rm tot}$ indeed remains a smooth function of α without exhibiting a singular behavior (though it decreases quickly) acrossing the critical α_c. Here the α_c is marked by a vertical dashed line, which has been previously determined[9,10] in terms of the ground state energy and the onset of a characteristic momentum Q_0 at $\alpha \geq \alpha_c$ [cf. Figs. 2(c) and 3(b)]. For comparison, $Z_{\rm tot}$ for the σ·t-J ladder is also presented in Fig. 1, in which there is no critical point (with $Q_0 = 0$) throughout the whole α regime.

A finite $Z_{\rm tot}$ only means that $|\Psi_G\rangle$ has a finite probability remaining in a *bare* hole state [cf. Eq. (4)]. However, to determine whether the injected hole behaves like a Bloch wave or not, one needs to further inspect Z_k. Here Z_k is found to be peaked at $k_0 = \pi$ [or $k_0 = 0$] for the t-J model at $\alpha < \alpha_c$ [or the σ·t-J model] as shown in Fig. 2(a) [or (b)]. The data presented in the insets of Figs. 2(a) and (b) can be well collapsed under a rescaling of k_x by $(k_x - k_0)N_x$ in the main panels. They clearly indicate that the doped hole behaves like a coherent Bloch wave that is well *quantized* in a finite size system [under an open boundary condition (OBC)]. In the large N_x limit, the ground state possesses a single momentum k_0, which satisfies the translation symmetry as expected.

At $\alpha > \alpha_c$, the momentum k_0 is split by Q_0 as $k_0^+ - k_0^- = Q_0$ for the t-J model. The emerging double-peak structure centered at $k_0^\pm$ is shown in the inset of Fig. 2(c) at $\alpha = 5 > \alpha_c$. The wave quantization under the OBC is no longer valid here, as clearly illustrated in the main panel of Fig. 2(c). Here many momenta (instead of two $k_0^\pm$) are involved in the large-N_x case, which implies a breakdown of the translation symmetry. As a matter of fact, the distribution of momenta strongly scatter around $k_0^\pm$ even under small changes of sample sizes, for example, $N_x = 192$, 200, 202, and 206, as shown in Fig. 2(d). It indicates that a large fluctuation may occur in the phase shift[1,13] of the wave due to strong scattering between the hole and spin background, which scrambles the momentum quantization of the wave under the OBC. By contrast, $Z_{\rm tot}$ as the summation of Z_k still converges quickly with the increase of N_x [cf. the inset of Fig. 1].

To further verify the breakdown of the Bloch wave behavior observed above, one can examine the corresponding real space distribution Z_j. In Figs. 3(a) and (b), Z_j and its Fourier transformation F_q are presented, respectively, which exhibit a sharp spatial oscillation characterized by Q_0 [cf. Fig. 3(b)] at $\alpha = 5$. Figure 3(a) further indicates another slower spatial modulation of a length scale λ, which corresponds to a continuous broadening around Q_0 in Fig. 3(b). It is consistent with the momentum smearing manifested in Z_k around $k_0^\pm$ in Figs. 2(c) and (d). Furthermore, the hole density distribution n_j^h and its Fourier transformation N_q are given in Figs. 3(c) and (d), which exhibit a charge modulation as well. In fact, by comparison it is easy to determine that the dominant contribution to the charge modulation in n_j^h comes from Z_j, i.e., the bare hole component of $|\Psi_G\rangle$. The incoherent length scale λ vs. N_x is plotted in the inset of Fig. 3(c).

It is noted that Z_k and Z_j are determined by the single hole propagator, which may be formally expressed as[12,13] $G_h(i,j;E) \propto \sum_{c_{ij}} \tau_{c_{ij}} P(c_{ij})$ where c_{ij} include all the paths of spins and the hole with the hole path connecting site i and j,

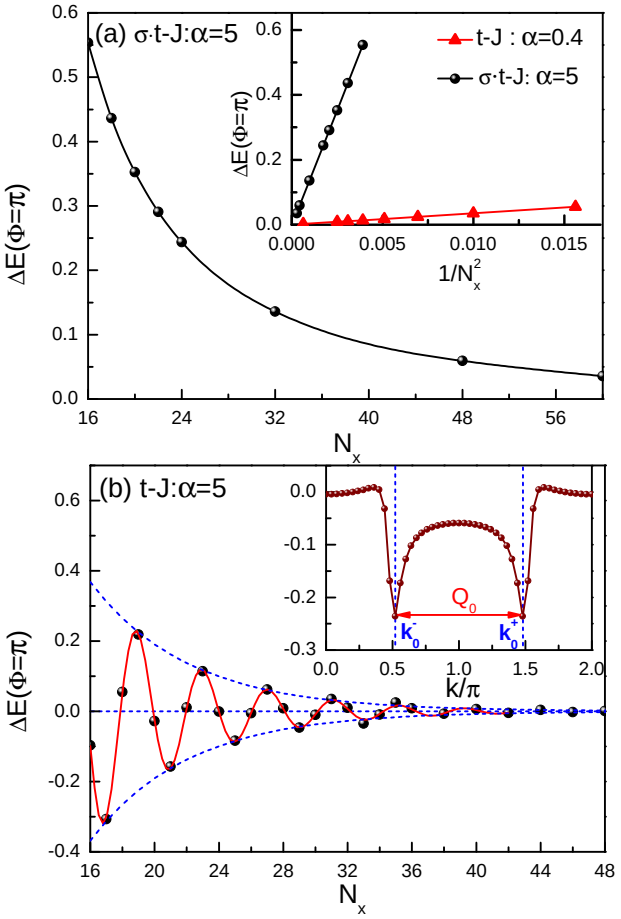

Fig. 4. (Color online). The energy change due to the charge response to an inserted flux $\Phi = \pi$ into the ring geometry of the ladder (see text). (a) The typical Bloch wave behavior ($\propto 1/N_x^2$) for the σ·t-J case and the t-J ladder at $\alpha < \alpha_c$ (the inset); (b) The non-Bloch-wave response at $\alpha > \alpha_c$ in the t-J case can be well fitted by Eq. (5), which directly relates the phase string effect as the underlying cause for charge incoherence and incommensurate momentum splitting (the inset) according to Eq. (6).

and the weight $P(c_{ij}) > 0$[14]. According to Eq. (2), one may show[10] that the momentum structure and the charge modulation come from $\tau_{c_{ij}} \sim \mathrm{e}^{i\mathbf{k}_0\cdot[\mathbf{r}_i-\mathbf{r}_j]+i\delta_{ij}}$, in which $\mathbf{k}_0\cdot[\mathbf{r}_i-\mathbf{r}_j]$ denotes an averaged $N_h^{\downarrow}(c_{ij})$ and the phase shift δ_{ij} captures the rest of many-body fluctuations around $\mathbf{k}_0 = \mathbf{k}_0^{\pm}$. The phase shift δ_{ij} is the source leading to the above breakdown of the Bloch wave behavior. As a matter of fact, by switching off τ_c in the σ·t-J model, all the modulations disappear in Z_j and n_j^h as indicated in Figs. 3(e) and (f).

Charge incoherence.— To probe the charge incoherence revealed by Z_k and Z_j at $\alpha > \alpha_c$, one may alternatively study the charge response to inserting a magnetic flux Φ into a ring of the ladder enclosed along the chain direction. Define the energy change $\Delta E_G^{\text{1-hole}} \equiv E_G^{\text{1-hole}}(\Phi = \pi) - E_G^{\text{1-hole}}(\Phi = 0)$, with $\Phi = 0$ corresponding to the periodic boundary condition (PBC) and $\Phi = \pi$ the anit-PBC for the hole[7,9]. For a Bloch-wave behavior of the doped hole, one expects[7,9] that $\Delta E_G^{\text{1-hole}} \propto 1/N_x^2$. Indeed, as confirmed by DMRG, this is true for the σ·t-J case [Fig. 4(a) and the inset] as well as the t-J model at $\alpha < \alpha_c$ [the inset of Fig. 4(a), $N_x = \text{even}$].

However, for the t-J case at $\alpha > \alpha_c$, the charge incoherence is clearly manifested as shown in Fig. 4(b) at $\alpha = 5$: $\Delta E_G^{\text{1-hole}}$ oscillates strongly with N_x, which can be fitted by

$$\Delta E_G^{\text{1-hole}}(t\text{-}J) \propto \left(\mathrm{e}^{ik_0^+ N_x} + \mathrm{e}^{ik_0^- N_x}\right) g(N_x)\,, \qquad (5)$$

where the incommensurate $k_0^{\pm}$ emerge as indicated in the inset of Fig. 4(b). Here the envelope function, $g(N_x)$, further gives rise to the broadening of the peaks $k_0^{\pm}$ as shown by its Fourier transformation in the inset of Fig. 4(b), which characterizes the incoherent scale of the charge.[15]

Analytically, a straightforward manipulation in terms of Eq. (1) gives rise to

$$\begin{aligned}\Delta E_G^{\text{1-hole}}(t\text{-}J) &= -\lim_{\beta\to\infty}\frac{1}{\beta}\ln\left(\frac{\mathcal{Z}_{t\text{-}J}(\Phi=\pi)}{\mathcal{Z}_{t\text{-}J}(\Phi=0)}\right)\\ &= 2\sum_{c_1}\tau_{c_1}\rho_{c_1} + 2\sum_{c_3}\tau_{c_3}\rho_{c_3} + \ldots\,, \qquad (6)\end{aligned}$$

while, for the σ·t-J model, $\Delta E_G^{\text{1-hole}}(\sigma t\text{-}J) = 2\sum_{c_1}\rho_{c_1} + 2\sum_{c_3}\rho_{c_3} + \ldots$[16]. Here, $\mathcal{Z}_{t\text{-}J}(\Phi = 0) \equiv \sum_\nu \mathcal{Z}_{t\text{-}J}^{(\nu)}$ and $\mathcal{Z}_{t\text{-}J}(\Phi = \pi) \equiv \sum_\nu (-1)^\nu \mathcal{Z}_{t\text{-}J}^{(\nu)}$ with $\mathcal{Z}_{t\text{-}J}^{(\nu)} \equiv \sum_{c_\nu}\tau_{c_\nu}\mathcal{W}[c_\nu]$, where ν denotes the winding number counting how many times the hole circumvents the ring, and $\rho_{c_\nu} \equiv \lim_{\beta\to\infty}\mathcal{W}[c_\nu]/(\beta\mathcal{Z}_{t\text{-}J}^{(0)}) > 0$. Therefore, Eq. (5) and Fig. 4 provide a direct measurement of $\sum_{c_1}\tau_{c_1}\rho_{c_1}$ in Eq. (6) at large N_x (note that $\nu > 1$ terms decay faster as N_x increases), which indeed gives rise to the incommensurate $k_0^{\pm}$ and relates an incoherence scale with the phase shift fluctuation in τ_{c_1}. These are indeed consistent with the picture previously obtained based on Z_k and Z_j.

Conclusions.— Doping into a gapped spin system is one of the simplest cases of doped Mott physics. Should the non-Bloch-wave behavior be fully validated for the one hole case, complemented by a strong pairing discovered[8] for the two hole case, an important understanding of the nature of strong correlation can be gained. Both DMRG simulations on the quasiparticle spectral weights, Z_k and Z_j, and the charge response to inserting a flux have given rise to a consistent picture in this work. Namely, the momentum splitting and charge modulations found[7,9,10] at $\alpha > \alpha_c$ cannot be simply reduced to a standing wave description of two counter-propagating Bloch waves[11]. Here, the hole loses its Bloch wave coherence intrinsically with involving a continuum of momenta, which indicates a spontaneous translational symmetry breaking. The microscopic origin due to τ_c in Eq. (2) (which is called the phase string effect[13] characterizing the long-range entanglement between the spins and the doped charge[17,18]) has been thus established. This mechanism has also been recently studied by a variational wave function approach[19], which can reproduce, e.g., α_c and Q_0, found by DMRG.

ACKNOWLEDGMENTS

Useful discussions with R.-Q. He, H.-C. Jiang, Y. Qi, J. Zaanen are acknowledged. This work is supported by Natural Science Foundation of China (Grant No. 11534007), National Program for Basic Research of MOST of China (Grant No. 2015CB921000), and US National Science Foundation Grant DMR-1408560.

[1] P. W. Anderson, *The Theory of Superconductivity in the High-Tc Cuprate Superconductors* (Princeton University Press, Princeton, NJ, 1997).

[2] P. A. Lee, N. Nagaosa, and X. G. Wen, Rev. Mod. Phys. **78**, 17 (2006).

[3] S. Schmitt-Rink, C. Varma, and A. Ruckenstein, Phys. Rev. Lett. **60**, 2793 (1988).

[4] C. Kane, P. Lee, and N. Read, Phys. Rev. B **39**, 6880 (1989).

[5] G. Martinez and P. Horsch, Phys. Rev. B **44**, 317 (1991).

[6] Z. Liu and E. Manousakis, Phys. Rev. B **44**, 2414 (1991).

[7] Z. Zhu, H.-C. Jiang, Y. Qi, C.-S. Tian, and Z.-Y. Weng, Sci. Rep. **3**, 2586 (2013).

[8] Z. Zhu, H.-C. Jiang, D. N. Sheng, and Z.-Y. Weng, Sci. Rep. **4**, 5419 (2014).

[9] Z. Zhu and Z.-Y. Weng, Phys. Rev. B **92**, 235156 (2015).

[10] Z. Zhu, C.-S. Tian, H.-C. Jiang, Y. Qi, Z.-Y. Weng, and J. Zaanen, Phys. Rev. B **92**, 35113 (2015).

[11] S. R. White, D. J. Scalapino, and S. A. Kivelson, Phys. Rev. Lett. **115**, 56401 (2015).

[12] K. Wu, Z. Y. Weng, and J. Zaanen, Phys. Rev. B **77**, 155102 (2008).

[13] D. N. Sheng, Y. C. Chen, and Z. Y. Weng, Phys. Rev. Lett. **77**, 5102 (1996).

[14] With E less than the ground state energy $E_G^{\text{1-hole}}$.

[15] Here one can fit $g \sim \mathrm{e}^{-\frac{N_x}{\xi}}$ with $\xi \sim 6.3$ as a characteristic incoherence (localization) length scale[7]. Note that ξ and $\lambda/2$ (~ 16), determined by the density distribution under OBC in Fig. 3(c), are related but not necessarily the same due to different ways of measurement. Further, the interference of the phase string under the PBC may be stronger at a relatively smaller N_x because there are more channels for the destructive interference involving the hole circumventing the closed ring. The results under PBC are expected to be eventually in full agreement with those under OBC at sufficiently larger N_x, which is beyond our current computing capability.

[16] By using the fact that each term is vanishingly small in the large N_x limit, cf. Fig. 4(a).

[17] J. Zaanen and B. J. Overbosch, Philos. Trans. R. Soc. A Math. Phys. Eng. Sci. **369**, 1599 (2011).

[18] Z.-Y. Weng, Front. Phys. **6**, 370 (2011).

[19] Q.-R. Wang, Z. Zhu, Y. Qi, and Z.-Y. Weng, arXiv:1509.01260.